

We are IntechOpen, the world's leading publisher of Open Access books Built by scientists, for scientists

6,900

Open access books available

186,000

International authors and editors

200M

Downloads

Our authors are among the

154

Countries delivered to

TOP 1%

most cited scientists

12.2%

Contributors from top 500 universities



WEB OF SCIENCE™

Selection of our books indexed in the Book Citation Index
in Web of Science™ Core Collection (BKCI)

Interested in publishing with us?
Contact book.department@intechopen.com

Numbers displayed above are based on latest data collected.
For more information visit www.intechopen.com



Molecular Descriptors and Properties of Organic Molecules

Amalia Stefaniu and Lucia Pintilie

Additional information is available at the end of the chapter

<http://dx.doi.org/10.5772/intechopen.72840>

Abstract

The main goal of this chapter is to reveal the importance of molecular structure analysis with specific computational tools using quantum chemistry methods based on density functional theory (DFT) with focus on pharmaceutical compounds. A wide series of molecular properties and descriptors related with chemical reactivity is discussed and compared for small organic molecules (e.g., quinolones, oxazolidinones). Structural and physicochemical information, important for quantitative structure-property relationships (QSPR) and quantitative structure-activity relationships (QSAR) modeling analysis, obtained using Spartan 14 software Wavefunction, are reported. Thus, by a computational procedure including energy minimization and predictive calculations, values of quantum chemical parameters and molecular properties related with electronic charge distribution are reported and discussed. Frontier molecular orbitals energy diagram and their bandgap provide indications about chemical reactivity and kinetic stability of the molecules. Derived parameters (ionization potential (I), electron affinity (A), electronegativity (χ), global hardness (η), softness (σ), chemical potential (μ) and global electrophilicity index (ω)) are given. Also, graphic quantities are reported: electrostatic potential maps, local ionization potential maps and LUMO maps, as visual representation of the chemically active sites and comparative reactivity of different constitutive atoms.

Keywords: quantum chemical parameters, linezolid, cadazolid, ciprofloxacin, molecular docking

1. Introduction

In recent years, prediction of chemical properties by computed tools becomes a useful and suitable way to analyze and compare wide libraries of compounds aiming to design and develop new molecules with higher biological activity and/or better and controlled chemical

behavior. Molecular design and prediction of molecular parameters using *ab initio* methods and mathematical modeling of physical and chemical properties are imperative steps in new scientific approaches for developing new drugs or advanced materials.

Due to the evolution of computing data storage and processor performance, molecular modeling rapidly integrates into the study of therapeutic molecules, due to the opportunities, it offers to solve relevant issues in a considerably short time without doing rebate from the accuracy of the predicted data.

The prediction of chemical properties and the assessment of chemical behavior in pseudo-physiological media by computational methods has become a necessary and fast tool to analyze and compare wide libraries of compounds in order to design and develop new molecules with important biological activity or to potentiate them or conduct their chemical behavior. Computed structural analysis and chemical parameters prediction using *ab initio* methods and mathematical modeling of physicochemical properties are imperative steps in these new approaches in developing drugs or advanced new materials.

Mathematical models are used to predict the strength of intermolecular interactions between drug candidates and their biological protein/enzyme target, allowing to identify the most probable binding mode and affinity and, finally, to explore the molecular mechanism or biochemical pathways.

Recent studies have been focused on the development of noncleavable dual-action molecules with antimicrobial activity. One of the noncleavable antibiotic hybrids is cadazolid, composed of a fluoroquinolone and an oxazolidinone core via a stable linker [1]. Regarding the mode of action, it was reported that cadazolid is acting as an oxazolidinone molecule but fails to demonstrate a substantial contribution from the fluoroquinolone function. Cadazolid behaves like a potent linezolid with a low systemic exposure and a high local concentration in the gastrointestinal tract [1]. Our theoretical studies focus on the characteristics, molecular properties and molecular docking simulations to identify and visualize the most likely interactions between ligands such as cadazolid, linezolid, quinolone and the receptor protein (*Staphylococcus aureus* ribosomal subunit, PDB ID: 4WFA).

2. Materials and methods

2.1. Prediction properties computation procedure

The properties calculations were carried out using Spartan 14 software Wavefunction, Inc. Irvine, CA, USA [2] on a PC with Intel(R) Core i5 at 3.2 GHz CPU. First, the 3D CPK models of the studied compounds were generated. Then, a systematic conformational search and analysis were performed to establish the more stable conformers of the three pharmacological compounds, presenting the energy minima. The lowest energy conformer was obtained using MMFF molecular mechanics model by refining the geometry for each studied molecule. On these structures, a series of calculations of molecular properties and topological descriptors were performed using density functional method [3], software algorithm hybrid B3LYP model (Becke's three

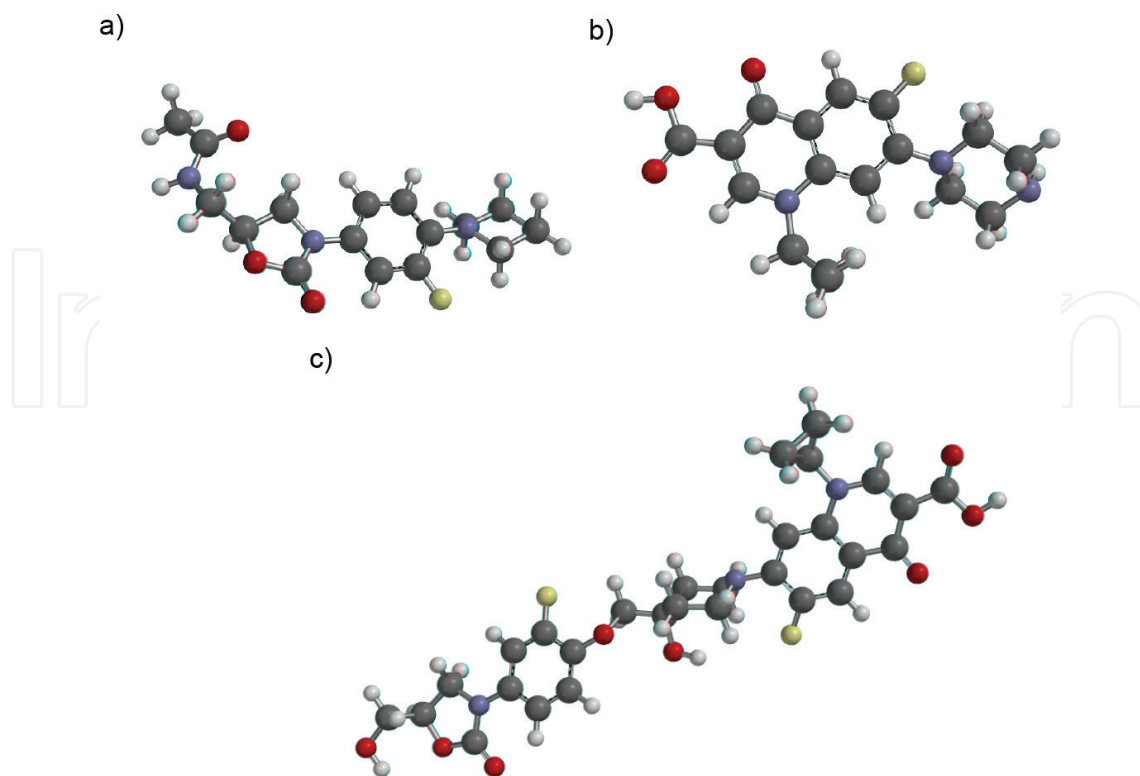


Figure 1. The optimized geometry of the pharmaceutical compounds: linezolid (a), ciprofloxacin (b) and cadazolid (c), ball and spoke representation.

parameter hybrid exchange functional with the Lee-Yang-Parr correlation functional) [3–5] and polarization basis set 6-31G* [2, 6] in vacuum, for equilibrium geometry at ground state.

2.2. Molecular docking simulations

The docking studies have been carried out using CLC Drug Discovery Workbench Software in order to predict the most possible type of interactions, the binding affinities and the orientation of the docked ligand (cadazolid, linezolid or quinolone) at the active site of *Staphylococcus aureus* ribosomal subunit [7]. The protein-ligand complex has been realized based on the X-ray structure of crystal structure of the large ribosomal subunit of *Staphylococcus aureus* in complex with linezolid, which was downloaded from the Protein Data Bank (PDB ID: 4WFA) [7]. Co-crystallized ligand linezolid (ZLD) was extracted and redocked into 4WFA fragment to validate the docking protocol. The docked ligands and their optimized geometry are illustrated in **Figure 1**, as ball and spoke representation.

3. Results and discussion

3.1. Molecular properties

Structural and physicochemical information, important for *quantitative structure-property relationships* (QSPR) and *quantitative structure-activity relationships* (QSAR) modeling analysis,

obtained using Spartan 14 software Wavefunction, are reported in **Table 1**. Thus, by a computational procedure, including energy minimization to obtain the most stable conformer for each studied structure and predictive calculations, values of quantum chemical parameters and molecular properties related with electronic charge distribution are obtained. Using the Calculate Molecular Properties Tool of Spartan 14 software, relevant properties of small molecules have been calculated, related with Lipinski's rule of five [8]. To be efficient drug candidates, the compounds must respect the following conditions: maximum five hydrogen bond donors (as total number of nitrogen-hydrogen and oxygen-hydrogen bonds); maximum 10 hydrogen bond acceptors (as total number of nitrogen and oxygen atoms); maximum molecular weight of 500 Da; the octanol-water partition coefficient (log P) value less than 5. In our study, the prediction log P coefficient is based on the XLOGP3-AA method [9]. These properties are important when several drug candidate compounds need to be analyzed, before their chemical synthesis, in order to evaluate their drug-likeness. In **Table 1** are listed the calculated molecular properties from CPK and from Wavefunction models for the three studied

	Linezolid	Ciprofloxacin	Cadazolid
Molecular properties			
Formula	C ₁₆ H ₂₀ FN ₃ O ₄	C ₁₇ H ₁₈ FN ₃ O ₃	C ₂₉ H ₂₉ F ₂ N ₃ O
Weight (amu)	337.351	331.347	585.560
Energy (au)	-1186.74569	-1148.36687	-2088.23350
Energy (aq) (au)	-1186.76351	-1148.36687	-2088.26194
Solvation E (kJ/mol)	-46.79	-57.23	-74.66
Dipole moment (Debye)	7.28	6.42	8.39
E HOMO (eV)	-5.28	-5.72	-5.88
E LUMO (eV)	-0.19	-1.33	-1.52
QSAR properties from CPK model			
Area (Å ²)	346.66	330.26	557.72
Volume (Å ³)	324.83	318.18	541.53
PSA (Å ²)	55.071	62.218	114.809
Ovality	1.52	1.47	1.74
QSAR properties from computed wavefunction			
Log P	0.58	1.32	2.37
HBD count	1	1	2
HBA count	6	5	9
Polarizability (10 ⁻³⁰ m ³)	66.52	66.15	84.27

Table 1. Predicted molecular properties for linezolid, ciprofloxacin and cadazolid, using DFT method, B3LYP model, 6-31G* basis set, in vacuum, for equilibrium geometry at ground state.

molecules obtained for the most stable conformer of each after geometry minimization: dipole moment, ovality, polarizability, the octanol-water partition coefficient ($\log P$), the number of hydrogen bond donors (HBDs) and acceptors (HBAs) and acceptor sites (HBAs), area, volume, polar surface area (PSA) and energies of frontier molecular orbitals (FMOs).

Area, volume and polar surface area have the same variation as the molecular weight, increasing in the following order: ciprofloxacin < linezolid < cadazolid.

The ovality index represents the deviation from the spherical form, considering its value 1 for spherical shape. From our calculations, we found the following variation of this parameter: 1.47 (ciprofloxacin) < 1.52 (linezolid) < 1.74 (cadazolid). Ovality index is related with molecular surface area and van der Waals volume, and it increases with the increase of structural linearity. The polarizability provides information about induction (polarization) interactions resulting from an ion or a dipole inducing a temporary dipole in an adjacent molecule. The same variation is observed for both polarizability and for the dipole moment.

The octanol-water partition coefficient ($\log P$) is related with the lipophilicity of compounds and is useful to predict the absorption of drugs across the intestinal epithelium.

$\log P$ values are calculated according to Ghose, Pritchett and Crippen method [10]. The criteria of Lipinski's rule of five [11], $\log P$ must be smaller than 5 for a good drug candidate, are based on the observation that the most orally absorbed compounds have $\log P < 5$. $\log P$ can be correlated with PSA when the potential drugs are evaluated according to Hughes et al. [12] who proposed the criteria as $\log P < 4$ and $PSA > 75 \text{ \AA}^2$.

Molecular orbitals energy diagrams and gap (ΔE) are obtained from the energetic level values (eV) of frontier molecular energy orbitals (FMNOs): HOMO—the *highest occupied molecular orbital* and LUMO—the *lowest unoccupied molecular orbital*.

The molecular frontier orbitals are important descriptors related to the reactivity of molecules. Thus the higher value refers to chemically stable molecules. The HOMO energy is linked to the tendency of a molecule to donate electrons to empty molecular orbitals with low energy of convenient molecules. The LUMO energy indicates the ability to accept electrons. The frontier molecular orbital density distribution of the studied therapeutic compounds is shown in **Figure 2** (for linezolid (a), ciprofloxacin (b) and cadazolid (c): HOMO (top) and LUMO (bottom)). Black and dark gray regions correspond to positive and negative values of the orbital.

The frontier orbital gap helps to characterize chemical reactivity and kinetic stability [13, 14] of the molecules. HOMO and LUMO determine the way in which it interacts with other species.

The obtained energy gap increases in the order: cadazolid < ciprofloxacin < linezolid (4.36 < 4.39 < 5.09). Consequently, among the three analyzed therapeutical compounds, linezolid presents the lowest reactivity (the most chemically stable) followed by ciprofloxacin and cadazolid (the most reactive).

Other derived quantum chemical parameters for the most stable conformers of linezolid, ciprofloxacin and cadazolid, such as ionization potential (I), electron affinity (A), electronegativity

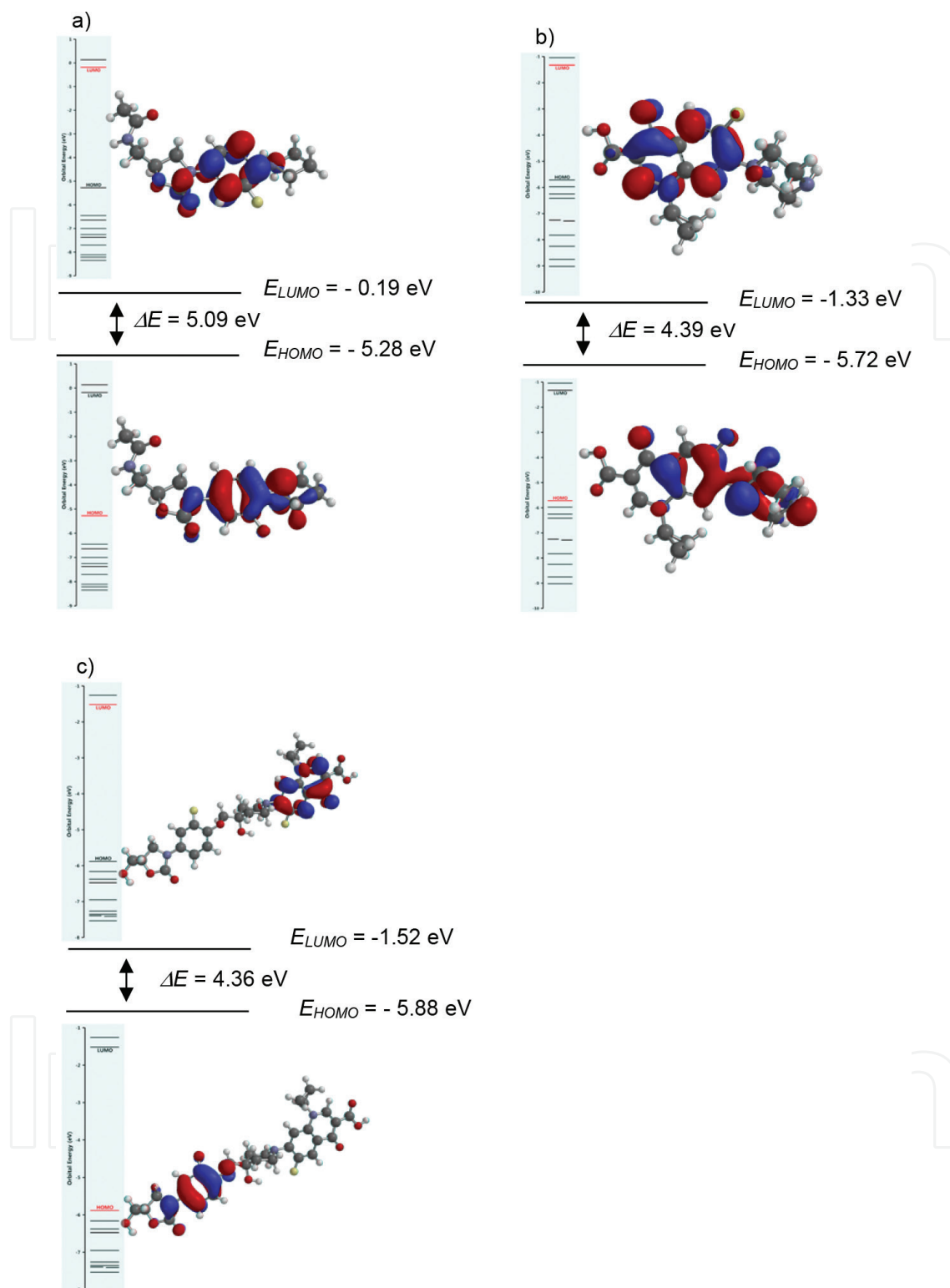


Figure 2. HOMO-LUMO plots (ground state) and energy diagram. HOMO-LUMO plots of (a) linezolid, (b) ciprofloxacin and (c) cadazolid.

(χ), global hardness (η), softness (σ), chemical potential (μ) and global electrophilicity index (ω), are obtained and listed in **Table 2**. Their values were derived from HOMO and LUMO energy diagram [15, 16], according to Koopmans' theorem [17, 18]. The ionization potential is defined as $I = -E_{HOMO}$ and the electron affinity as $A = -E_{LUMO}$.

Quantum parameters	Linezolid	Ciprofloxacin	Cadazolid
E_{HOMO} (eV)	-5.2763	-5.7170	-5.8839
E_{LUMO} (eV)	-0.1856	-1.3262	-1.5517
ΔE ($E_{\text{HOMO}} - E_{\text{LUMO}}$) (eV)	5.0907	4.3908	4.3670
$I = -E_{\text{HOMO}}$ (eV)	5.2763	5.7170	5.8839
$A = -E_{\text{LUMO}}$ (eV)	0.1856	1.3262	1.5517
$\chi = (I + A)/2$ (eV)	2.7309	3.5216	3.7178
$\eta = (I - A)/2$ (eV)	2.5453	2.1954	2.1661
$\sigma = 1/\eta$	2.0829	2.6041	2.7163
$\mu = (E_{\text{HOMO}} + E_{\text{LUMO}})/2$	-2.7309	-3.5216	-3.7178
$\omega = \mu^2/2\eta$	-1.4650	2.4362	3.1905

Table 2. Calculated quantum chemical parameters of the studied compounds.

3.1.1. Graphical quantities: electrostatic potential, local ionization potential and |LUMO| maps

These graphical quantities provide a visual representation of the chemically active sites and comparative local reactivity of analyzed structures.

Molecular electrostatic potential (MEP) is used to investigate the chemical reactivity of a molecule. The MEP is especially important for the identification of the reactive sites of nucleophilic or electrophilic attack in hydrogen bonding interactions and for the understanding of the process of biological recognition. The electrostatic potential map for all three compounds shows hydrophilic regions (negative and positive potentials) and hydrophobic regions (neutral). Their variations and local values are illustrated in **Figure 3**. For linezolid (**Figure 3a**), the negative potentials are localized over oxygen atoms, presenting values: -154, -156 and -160 kJ/mol. The positive electrostatic potential presents a maximum value of 234 kJ/mol. For ciprofloxacin (**Figure 3b**), the negative values vary between -209 and -166 kJ/mol, while positive values are lower than those found for linezolid (194 kJ/mol). For cadazolid (**Figure 3c**), the negative regions present values between -219 and -159 kJ/mol, and positive regions vary between 190 and 214 kJ/mol.

Local ionization potential map (LIPM) is represented in **Figure 4** for linezolid (a), ciprofloxacin (b) and cadazolid (c). The ionization potential represents an overlay of the energy of electron removal (ionization) on the electron density, being particularly useful to assess chemical reactivity and selectivity, in terms of electrophilic reactions.

|LUMO| map is an indicator of nucleophilic addition and it is provided by an overlay of the absolute value of the lowest unoccupied molecular orbital (LUMO) on the electron density.

Figure 5 illustrates the graphical representation for |LUMO| maps for linezolid (a), ciprofloxacin (b) and cadazolid (c).

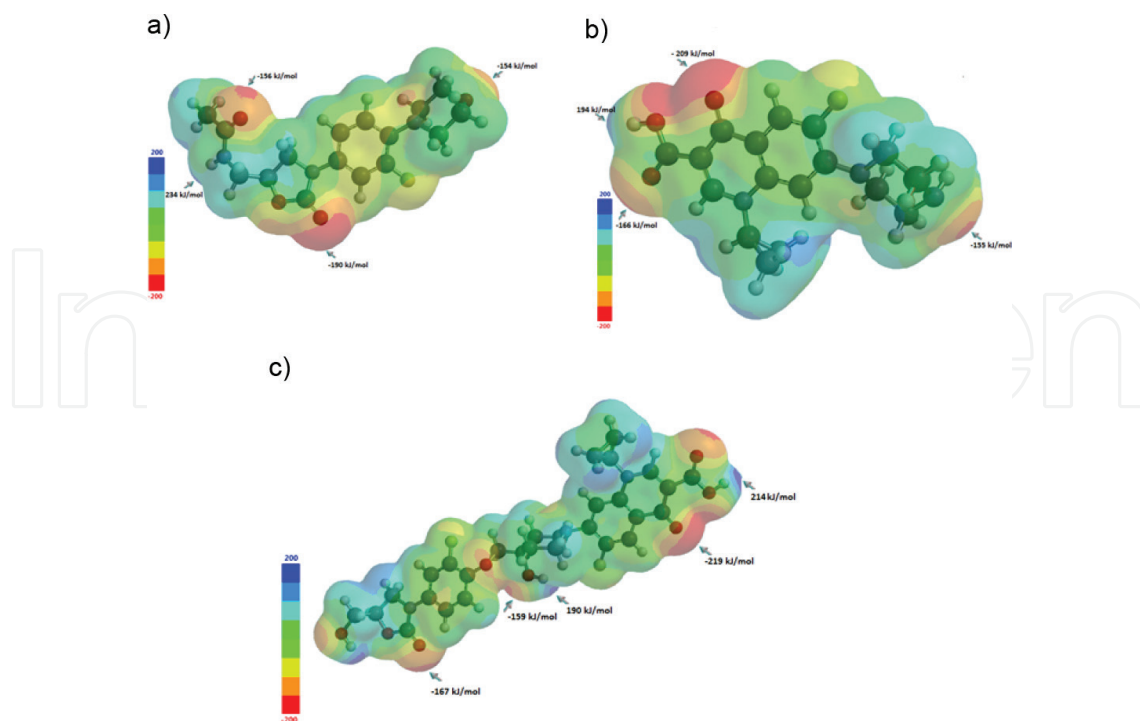


Figure 3. Electrostatic potential map (EPM) of linezolid (a), ciprofloxacin (b) and cadazolid (c), ball and spoke representation.

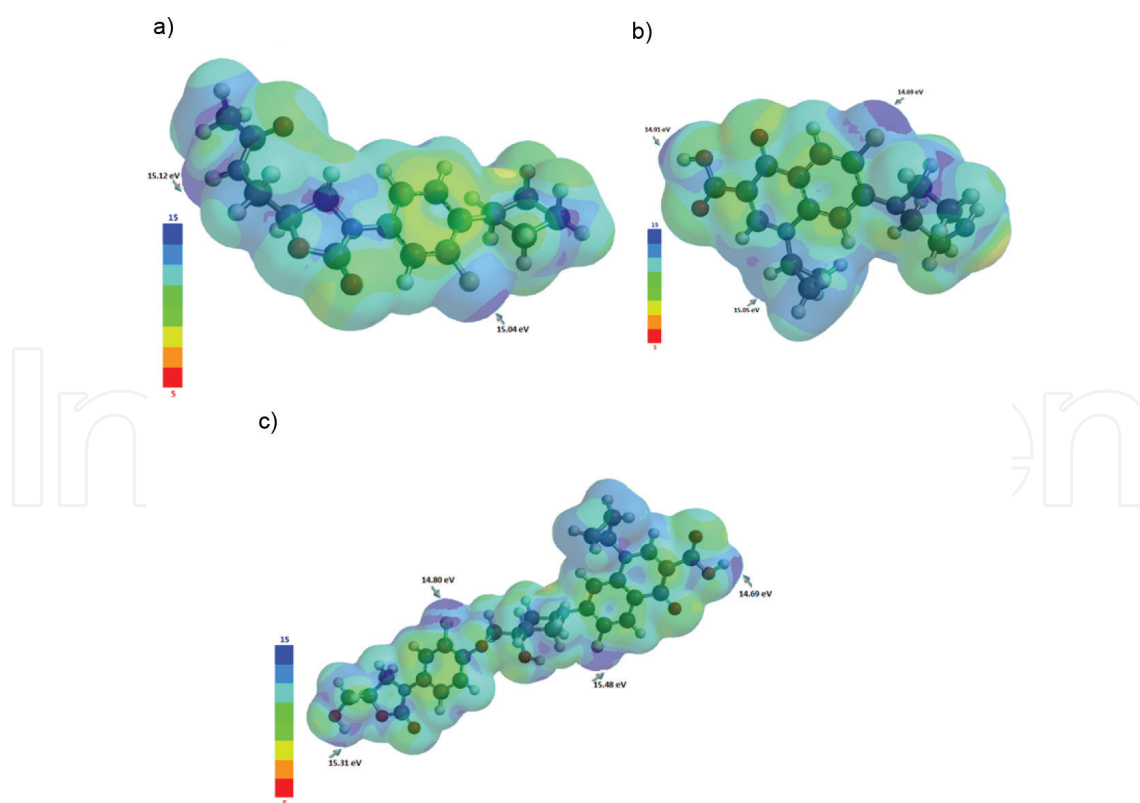


Figure 4. Local ionization potential map (LIPM) of (a) linezolid, (b) ciprofloxacin and (c) cadazolid.

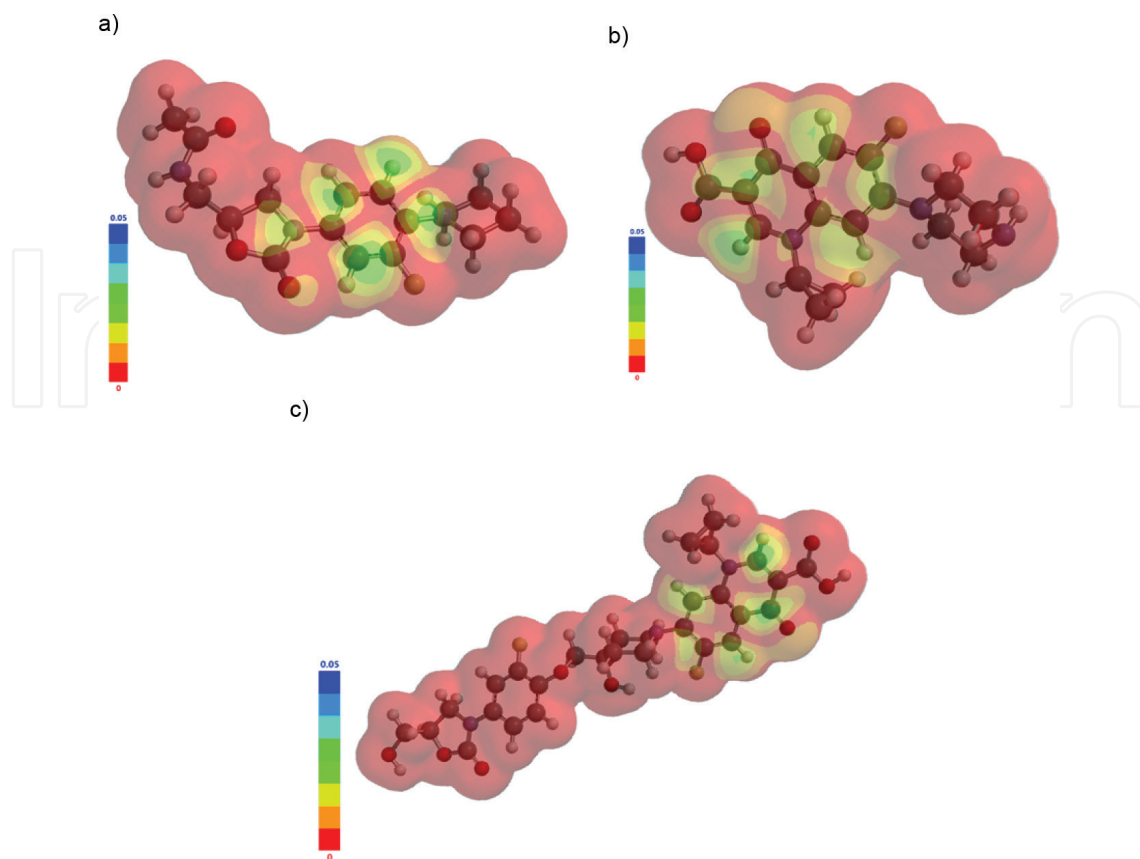


Figure 5. |LUMO| map (a) linezolid, (b) ciprofloxacin and (c) cadazolid.

The values of energetic intermediary levels of HOMO and LUMO orbitals for the studied compounds, predicted with B3LYP, 6-31G* algorithm are listed in **Table 3**.

Contribution of other occupied (HOMO{-1}-HOMO{-9}) and unoccupied molecular orbitals (LUMO{+1}) at UV VIS allowed transitions are presented in **Table 4** for linezolid, **Table 5** for ciprofloxacin and **Table 6** for cadazolid.

3.2. Molecular docking simulations

The docking score is a measure of the antimicrobial activity of the studied molecules. The 4WFA fragment, imported from PDB, was chosen for docking study because of the presence in its crystallographic structure of co-crystallized linezolid (ZLD). The crystal structure validated by X-ray diffraction contains a large ribosomal subunit of *Staphylococcus aureus* in complex with linezolid (ZLD). The polymeric chains also include 36 unique types of molecules: RNA chain 23S rRNA; RNA chain 5S rRNA, 50S ribosomal proteins L2-L6, 50S ribosomal proteins L13-L36, molecule N-[(5S)-3-(3-fluoro-4-morpholin-4-ylphenyl)-2-oxo-1,3-oxazolidin-5-yl]methyl]acetamide (ZLD-linezolid), molecule (4S)-2-methyl-2,4-pentanediol (MPD), magnesium ion, manganese(ii) ion, sodium ion, molecule 4-(2-hydroxyethyl)-1-piperazine ethanesulfonic acid (EPE), spermidine (SPD) and ethanol, as deposited in PDB on 2014-09-14, with the ID 4WFA [19].

Orbital	Linezolid	Ciprofloxacin	Cadazolid
HOMO	-5.3	-5.7	-5.9
HOMO{-1}	-6.5	-6.0	-6.2
HOMO{-2}	-6.6	-6.3	-6.4
HOMO{-3}	-7.0	-6.4	-6.5
HOMO{-4}	-7.3	-7.2	-7.0
HOMO{-5}	-7.4	-7.3	-7.3
HOMO{-6}	-7.7	-7.8	-7.4
HOMO{-7}	-8.1	-8.3	-7.4
HOMO{-8}	-8.2	-8.8	-7.4
HOMO{-9}	-8.4	-9.0	-7.5
LUMO	-0.2	-1.3	-1.5
LUMO{+1}	0.1	-1.0	-1.3

HOMO and LUMO orbitals and their values are in bold characters to highlight that they are the frontier molecular orbitals, and their values occur in the calculus of the energy gap (ΔE) and other quantum molecular parameters related with the global chemical reactivity of molecules.

Table 3. Linezolid, ciprofloxacin and cadazolid energetic levels (eV) of intermediary molecular orbitals (MO).

Wavelength (nm)	Strength	MO component	Contribution
211.68	0.1076	HOMO-1 \rightarrow LUMO+1	43%
		HOMO-1 \rightarrow LUMO	38%
		HOMO-2 \rightarrow LUMO	13%
223.10	0.0605	HOMO-1 \rightarrow LUMO	51%
		HOMO-1 \rightarrow LUMO+1	25%
255.34	0.3172	HOMO \rightarrow LUMO+1	65%
		HOMO \rightarrow LUMO	20%
274.49	0.1237	HOMO \rightarrow LUMO	70%
		HOMO \rightarrow LUMO+1	18%

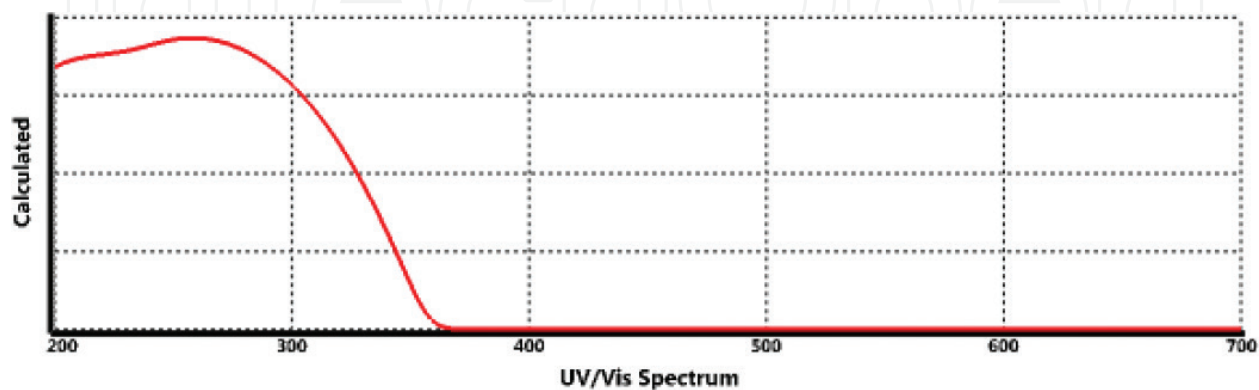


Table 4. Linezolid UV/Vis allowed transitions.

Wavelength (nm)	Strength	MO component	Contribution
277.36	0.3043	HOMO-1 → LUMO+1	33%
		HOMO-3 → LUMO	19%
		HOMO-1 → LUMO	16%
		HOMO → LUMO+1	16%
279.79	0.0653	HOMO-1 → LUMO+1	36%
		HOMO → LUMO+1	33%
		HOMO-1 → LUMO	14%
292.77	0.0014	HOMO-2 → LUMO+1	92%
300.49	0.0204	HOMO-1 → LUMO	51%
		HOMO → LUMO+1	43%
318.08	0.0927	HOMO → LUMO	84%
334.30	0.0023	HOMO-2 → LUMO	88%

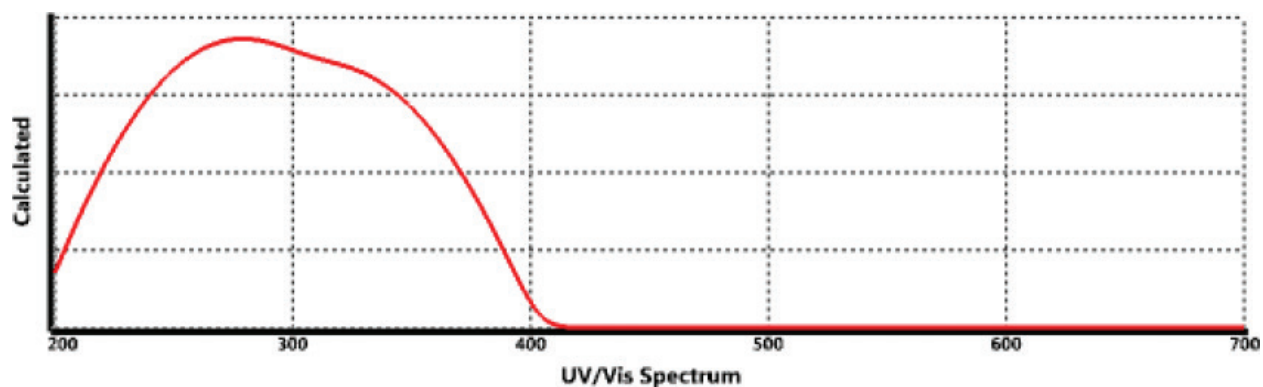


Table 5. Ciprofloxacin UV/Vis allowed transitions.

Wavelength (nm)	Strength	MO component	Contribution
286.51	286.51	HOMO-1 → LUMO	82%

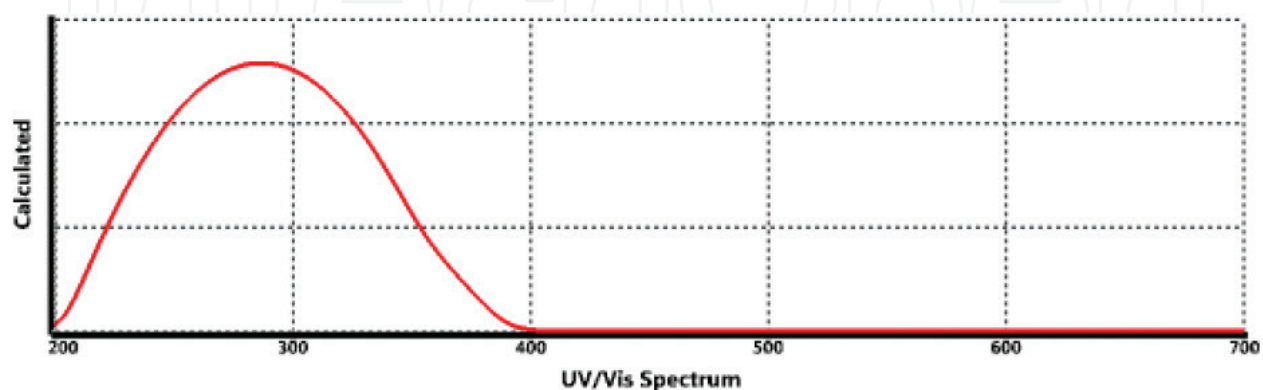


Table 6. Cadazolid UV/Vis allowed transitions.

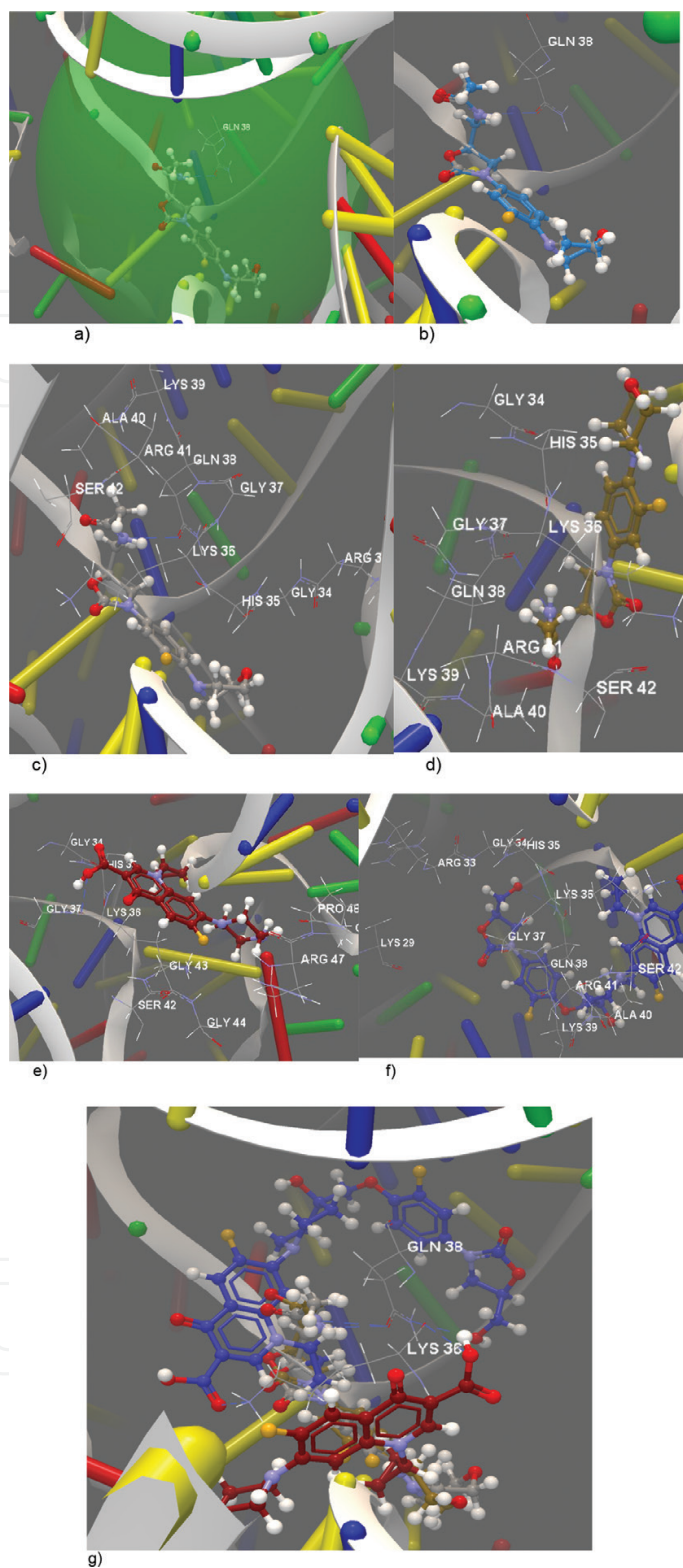


Figure 6. Molecular docking results on linezolid, ciprofloxacin and cadazolid with 4WFA receptor. (a) Active binding site of 4WFA. (b) Docking validation of co-crystallized ZLD. (c) Interacting group and hydrogen bonds between the residues of the GLN 38 and the co-crystallized ZLD. (d) Interacting group of linezolid and hydrogen bonds between the residues of the GLN 38 and the linezolid. (e) Interacting group of ciprofloxacin and hydrogen bonds between the residues of LYS 36 and ciprofloxacin. (f) Interacting group of cadazolid and hydrogen bonds between the residues of LYS 36 and GLN 38 and cadazolid. (g) Docking pose of the four ligands: co-crystallized ZLD (light gray), linezolid (gray), ciprofloxacin (black) and cadazolid (dark gray) with 4WFA.

The docking simulations comprise the following steps: ligands preparation and calculate molecular properties, setup the binding site of the receptor protein, dock ligands, validation of docking, analyze and measure the interactions of the ligand with the amino acid group, analyze docking results in terms of docking score and root-mean-square deviation (RMSD). The docking studies aim to predict the binding modes, the binding affinities and the orientation of the docked ligands. In **Figure 6**, the docking results are illustrated; the active binding site of 4WFA (a), docking validation of co-crystallized ZLD (b), interacting group and hydrogen bonds between the residues of GLN 38 and co-crystallized ZLD (c), interacting group of linezolid and hydrogen bonds between the residues of GLN 38 and linezolid (d), interacting group of ciprofloxacin and hydrogen bonds between the residues of LYS 36 and ciprofloxacin (e), the interacting group of cadazolid and hydrogen bonds between the residues of LYS 36 and GLN 38 and cadazolid (f), docking pose of the four ligands: co-crystallized ZLD (gray), linezolid (brown), ciprofloxacin (red) and cadazolid (blue) with 4WFA (g).

The results of molecular docking studies reveal the docking score -49.75 (RMSD: 2.65 \AA) for cadazolid and shows the occurrence of two hydrogen bonds with GLN 38 (2.930 \AA) and LYS 36 (3.020 \AA). Cadazolid forms a hydrogen bond with the same amino acid as linezolid (the first oxazolidinone introduced into therapeutics) and a hydrogen bond with the same amino acid as ciprofloxacin (second-generation fluoroquinolone) (**Table 7**). The obtained docking score resulted from the contributions of hydrogen bond score, metal interaction score and steric interaction score.

3.2.1. Drug-likeness of the studied therapeutical compounds

As seen from the analysis of docked ligands, from **Table 8**, cadazolid presents two violations of the parameters involved in Lipinski's rule of five: the mass and the number of hydrogen acceptors (11), although the docking score is better, yet the RMSD has the higher value. These results can be correlated with cadazolid behavior, acting more likely as an oxazolidinone. Also, cadazolid presents the higher values of the water-octanol coefficient, from calculations made not only with CLC Drug Discovery Workbench software but also with Spartan software,

Compound	Score/RMSD	Interacting group	Hydrogen bond	Bond length (\AA)
Linezolid-co-crystallized (ZLD)	$-34.55/1.66$	ARG 33(I), GLY 34(I), HIS 35(I), LYS 36(I), GLY 37(I), GLN 38(I), LYS 39(I), ARG 41(I), ALA 40(I), SER 42(I)	N sp^2 (N14) – O sp^2 from GLN 38(I)	2.917
Linezolid	$-37.97/0.22$	GLY 34(I), HIS 35(I), LYS 36(I), GLY 37(I), GLN 38(I), LYS 39(I), ARG 41(I), ALA 40(I), SER 42(I)	N sp^2 (N14) – O sp^2 from GLN 38(I)	2.989
Ciprofloxacin	$-36.79/0.19$	GLY 34(I), GLY 37(I), LYS 36(I), SER 42(I), HIS 35(I), GLY 43(I), PRO 48(I), GLY 49(I)	O sp^3 (O2) – O sp^2 from LYS 36(I)	2.996
Cadazolid	$-49.75/2.65$	LYS 29(I), ARG 33(I), GLY 34(I), HIS 35(I), LYS 36(I), GLY 37(I), GLN 38(I), ARG 41(I), LYS(39(I), ALA 40(I), SER 42(I).	O sp^2 (O9) – N sp^2 from LYS 36(I)	3.020
			O sp^3 (O8) – N sp^2 from GLN 38(I)	2.930

Table 7. The list of intermolecular interactions between the ligands docked with 4WFA using CLC Drug Discovery Workbench software.

Compound	Atoms	Weight [Da]	Flexible bonds	Lipinski violations	Hydrogen donors	Hydrogen acceptors	Log P
Linezolid-co-crystallized (ZLD)	44	337.35	4	0	1	7	1.29
Linezolid	44	337.35	4	0	1	7	1.29
Ciprofloxacin	42	331.34	3	0	2	6	0.84
Cadazolid	71	585.55	8	2	3	11	4.14

Table 8. Ligands properties, computed with CLC Drug Discovery Workbench software.

both using different methods for the calculation of this parameter. Also, the differences in predicted values of log P can be attributed to the fact that Spartan software considers a rigorous conformational analysis before calculating the molecular properties. The calculated values with Spartan software are obtained only for the conformer with the lower energy.

4. Conclusions

Ab initio computation to molecular properties prediction and *in silico* molecular docking simulations help to evaluate the biological activity of several compounds and to assess their therapeutical potential.

Ciprofloxacin and linezolid can be used as reference compounds for their antimicrobial activity in order to analyze several derivatives of their class as drug candidates. Ciprofloxacin and linezolid fulfill both Lipinski and Hughes et al. rules about drug likeness, confirmed also by their use in therapeutics. Spartan 14 and CLC Drug Discovery Workbench Software offer the possibility of a deep conformational analysis and to obtain accurate predictive property data.

Acknowledgements

This study has been financed through the NUCLEU Program, which is implemented with the support of ANCSI, project no. PN 16-27 01 01 of the National Institute of Chemical-Pharmaceutical Research & Development—Bucharest, Romania.

Author details

Amalia Stefaniu* and Lucia Pintilie

*Address all correspondence to: astefaniu@gmail.com

National Institute of Chemical - Pharmaceutical Research and Development, ICCF
Bucharest, Romania

References

- [1] Ma Z, Lynch AS. Development of a dual-acting antibacterial agent (TNP-2092) for the treatment of persistent bacterial infections. *Journal of Medicinal Chemistry*. 2016;**59**: 6645-6657
- [2] Shao Y, Molnar LF, Jung Y, Kussmann J, Ochsenfeld C, Brown ST, Gilbert ATB, Slipchenko LV, Levchenko SV, O'Neill DP, DiStasio RA, Lochan RC, Wang T, Beran GJO, Besley NA, Herbert JM, Lin CY, Van Voorhis T, Chien SH, Sodt A, Steele RP, Rassolov VA, Maslen PE, Korambath PP, Adamson RD, Austin B, Baker J, Byrd EFC, Dachsel H, Doerksen RJ, Dreuw A, Dunietz BD, Dutoi D, Furlani TR, Gwaltney SR, Heyden A, Hirata S, Hsu CP, Kedziora G, Khalliulin RZ, Klunzinger P, Lee AM, Lee MS, Liang WZ, Lotan I, Nair N, Peters B, Proynov EI, Pieniazek PA, Rhee YM, Ritchie J, Rosta E, Sherrill CD, Simmonett AC, Subotnik JE, Woodcock HL, Zhang W, Bell AT, Chakraborty AK, Chipman DM, Keil FJ, Warshel A, Hehre WJ, Schaefer HF, Kong J, Krylov AI, PMW G, Head-Gordon M. Advances in methods and algorithms in a modern quantum chemistry program package. *Physical Chemistry Chemical Physics*. 2006;**8**(27):3172-3191
- [3] Parr RG, Yang W. *Density Functional Theory of Atoms and Molecules*. Oxford: Oxford University Press; 1989
- [4] Lee C, Yang W, Parr RG. Development of the Colle-Salvetti correlation-energy formula into a functional of the electron density. *Physical Review B*. 1988;**37**:785-789
- [5] Becke AD. Density functional thermochemistry. III. The role of exact exchange. *The Journal of Chemical Physics*. 1993;**98**:5648-5652
- [6] Hehre WJ. *A Guide to Molecular Mechanics and Quantum Chemical Calculations*. Irvine, CA: Wavefunction Inc.; 2003
- [7] Eyal Z, Matzov D, Krupkin M, Wekselman I, Paukner S, Zimmerman E, Rozenberg H, Bashan A, Yonath A. Structural insights into species-specific features of the ribosome from the pathogen *Staphylococcus aureus*. *Proceedings of the National Academy of Sciences of the United States of America*. 2015;**112**:E5805-E5814. DOI: 10.1073/pnas.1517952112
- [8] Lipinski CA, Lombardo F, Dominy BW, Feeney PJ. Experimental and computational approaches to estimate solubility and permeability in drug discovery and development settings. *Advanced Drug Delivery Reviews*. 2001;**46**:3-26. DOI: 10.1016/S0169-409X(00)00129-0
- [9] Cheng T, Zhao Y, Li X, Lin F, Xu Y, Zhang X, Li Y, Wang R. Computation of octanol-water partition coefficients by guiding an additive model with knowledge. *Journal of Chemical Information and Modeling*. 2007;**47**:2140-2148. DOI: 10.1021/ci700257y
- [10] Arup K, Ghose AK, Pritchett A, Crippen GM. Atomic physicochemical parameters for three-dimensional structure directed quantitative structure-activity relationships. III: Modeling hydrophobic interactions. *Journal of Computational Chemistry*. 1988; **9**:80-90

- [11] Lipinski CA, Lombardo F, Dominy BW, Feeney PJ. Experimental and computational approaches to estimate solubility and permeability in drug discovery and development settings. *Advanced Drug Delivery Reviews*. 1997;**23**:3-25
- [12] Hughes JD, Blagg J, Price DA, Bailey S, Decrescenzo GA, Devraj RV, et al. Physicochemical drug properties associated with in vivo toxicological outcomes. *Bioorganic & Medicinal Chemistry Letters*. 2008;**18**(17):4872-4875
- [13] Alam MJ, Ahmad S. Anharmonic vibrational studies of L-aspartic acid using HF and DFT calculations. *Spectrochimica Acta A: Molecular and Biomolecular Spectroscopy*. 2012; **96**:992-1004
- [14] Demir P, Akman F. Molecular structure, spectroscopic characterization, HOMO and LUMO analysis of PU and PCL grafted onto PEMA-co-PHEMA with DFT quantum chemical calculations. *Journal of Molecular Structures*. 2017;**1134**:404-415
- [15] Zarrouk A, Zarrok H, Salghi R, Hammouti B, Al-Dey Ab SS, Touzani R, Bouachrine M, Warad I, Hadda TB. A theoretical investigation on the corrosion inhibition of copper by quinoxaline derivatives in nitric acid solution. *International Journal of Electrochemical Science*. 2012;**7**:6353-6364
- [16] Wang H, Wang X, Wang H, Wang L, Liu A. DFT study of new bipyrazole derivatives and their potential activity as corrosion inhibitors. *Journal of Molecular Modeling*. 2007; **13**(1):147-153
- [17] Sastri VS, Perumareddi JR. Molecular orbital theoretical studies of some organic corrosion inhibitors. *Corrosion Science*. 1997;**53**(8):617-622
- [18] Yankova R, Genieva S, Halachev N, Dimitrova G. Molecular structure, vibrational spectra, MEP, HOMO-LUMO and NBO analysis of $\text{Hf}(\text{SeO}_3)(\text{SeO}_4)(\text{H}_2\text{O})_4$. *Journal of Molecular Structure*. 2016;**1106**:82-88
- [19] Eyal Z, Matzov D, Krupkin M, Wekselman I, Zimmerman E, Rozenberg H, Bashan A, Yonath AE. The crystal structure of the large ribosomal subunit of *Staphylococcus aureus* in complex with linezolid-deposited PDB as 4WFA. 2014